Hydration and Molecular Motions in Synthetic Phytanyl-Chained Glycolipid Vesicle Membranes

Teruhiko Baba,* Hiroyuki Minamikawa,† Masakatsu Hato,* and Tetsurou Handa‡
*Nanotechnology Research Institute and †Research Center of Nanoarchitectonics, AIST, Tsukuba, Ibaraki 305-8565; and ‡Graduate School of Pharmaceutical Sciences, Kyoto University, Sakyo-ku, Kyoto 606-8501, Japan

ABSTRACT Proton permeation rates across membranes of a synthetic branch-chained glycolipid, 1,3-di-*O*-phytanyl-2-*O*-(β-D-maltotriosyl)glycerol ($Mal_3(Phyt)_2$) as well as a branch-chained phospholipid, diphytanoylphosphatidylcholine (DPhPC) were lower than those of straight-chained lipids such as egg yolk phosphatidylcholine (EPC) by a factor of ~4 at pH 7.0 and 25°C. To examine whether degrees of water penetration and molecular motions in $Mal_3(Phyt)_2$ membranes can account for the lower permeability, nanosecond time-resolved fluorescence spectroscopy was applied to various membranes of branch-chained lipids ($Mal_3(Phyt)_2$, DPhPC, and a tetraether lipid from an extremely thermoacidophilic archaeon *Thermoplasma acidophilum*), as well as straight-chained lipids (EPC, 1-palmitoyl-2-oleoyl-phosphatidylcholine (POPC), and digalactosyldiacylglycerol (DGDG)) using several fluorescent lipids. Degrees of hydration of glycolipids, $Mal_3(Phyt)_2$, and DGDG were lower than those of phospholipids, EPC, POPC, and DPhPC at the membrane-water interfaces. DPhPC showed the highest hydration among the lipids examined. Meanwhile, rotational and lateral diffusive motions of the fluorescent phospholipid in branch-chained lipid membranes were more restricted than those in straight-chained ones. The results suggest that the restricted motion of chain segments rather than the lower hydration accounts for the lower proton permeability of branch-chained lipid membranes.

INTRODUCTION

Archaea inhabit under extreme conditions such as very high temperature, low pH, or very high salt concentration; therefore, their lipid membranes are considered to be chemically and physically stable. These lipids are characterized by their molecular structure: ether links between glyceryl and highly branched hydrophobic chain (isopranyl chain) moieties and have been classified into two types: diethers (monopolar lipids) and tetraethers (bipolar lipids). The latter lipids are found in extremely thermoacidophilic archaea, e.g., the polar lipid of fraction E (PLFE) from *Sulfolobus acidocaldarius* and the main polar lipid (MPL, see Fig. 1) from *Thermoplasma acidophilum*, the membranes of which are stable and show exceptionally low permeabilities to proton and other ionic solutes (Elferink et al., 1992, 1994; Choquet et al., 1994; Freisleben et al., 1995; Gambacorta et al., 1995; Van de Vossenberg et al., 1998; Komatsu and Chong, 1998). The other lipids, diethers are found in methanogenic archaea and halophilic archaea (Stewart et al., 1990; Choquet et al., 1994; Gambacorta et al., 1995; Van de Vossenberg et al., 1998), the membranes of which are also considered to be stable and exhibit low permeability (Stewart et al., 1990; Yamauchi et al., 1992, 1993; Dannenmuller et al., 2000). Because the barrier function of membranes is critical for the functioning of cell or intracellular organelles, where a proton motive force is established (Van de Vossenberg et al., 1998), archaeal lipid membranes are thought to be useful in avoiding short circuiting of the proton gradient and therefore to be promising for reconstitution matrices of various functional proteins, which generate or consume the proton motive force. It is of great interest to apply archaeal lipids to biochemical or biotechnological materials, and accordingly several trials have been made using tetraethers (Elferink et al., 1992; Choquet et al., 1994; Freisleben et al., 1995; Gambacorta et al., 1995), however, these lipids are not readily available in sufficient amounts and are often mixtures of heterogeneous lipids.

We recently proposed a series of 1,3-di-*O*-phytanyl-2-*O*-(β-glycosyl)glycerols ($Glc(Phyt)_2$, $Mal_N(Phyt)_2$ ($N = 2, 3, 5$); N is the number of glucose residue in the headgroup) as model archaeal monopolar lipids (Minamikawa and Hato, 1997; Hato et al., 1999). Among the synthetic glycolipids, $Mal_3(Phyt)_2$ (Fig. 1) forms stable planar or vesicle membranes suitable for functional reconstitution of labile membrane protein complexes such as photosystem II (Baba et al., 1999a,b). In addition, compared with planar lipid membranes from soybean phospholipids, those from $Mal_3(Phyt)_2$ exhibited 4- to 6-fold lower conductance, i.e., lower ion permeability. The conductance observed for $Mal_3(Phyt)_2$ was the same as that for a synthetic model archaeal phospholipid diphytanoylphosphatidylcholine (DPhPC; Fig. 1) (Baba et al., 1999b). $Mal_3(Phyt)_2$ therefore looks promising for construction of an artificial energy-conversion membrane system containing functional proteins involved in the generation or consumption of the proton motive force.

In the present study, we intended to obtain insights into the physicochemical properties of $Mal_3(Phyt)_2$ membranes in connection with their low proton permeability. Up to now, the factors governing proton permeability have been extensively discussed: water penetration into membranes is considered as the first step for proton permeation (Nagle,

Received for publication 4 June 2001 and in final form 7 September 2001.
Address reprint requests to Teruhiko Baba, Bio-Nanomaterial and Surface Interactions Group, Nanotechnology Research Institute, AIST, AIST Tsukuba Central 5, Tsukuba, Ibaraki 305-8565, Japan. Tel: 81–298-61–9327; Fax: 81–298-61–6232; E-mail: t-baba@aist.go.jp.

0006-3495/01/12/3377/10 $2.00

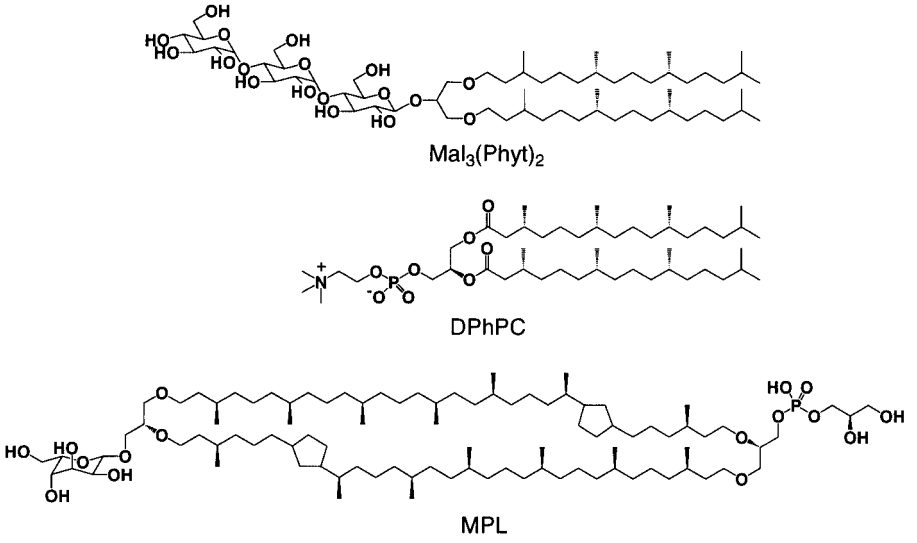

FIGURE 1 Chemical structures of monopolar lipids $Mal_3(Phyt)_2$, DPhPC, and the proposed chemical structure of the bipolar lipid MPL derived from *Thermoplasma acidophilum* (adapted from Swaine et al., 1997).

1987; Deamer and Nichols, 1989; Haines, 1994; Paula et al., 1996; Marrink et al., 1996) and membrane packing as well as motional freedom in membranes are considered to influence the permeability. In the case of tetraethers, low proton permeability was ascribed to rigid and tight membrane packing, preventing water penetration into membranes (Elferink et al., 1992; Komatsu and Chong, 1998; Khan and Chong, 2000; Gabriel and Chong, 2000). We applied nanosecond time-resolved fluorescence spectroscopy to $Mal_3(Phyt)_2$ membranes using several fluorescent probes and examined whether degrees of water penetration into $Mal_3(Phyt)_2$ membranes or molecular motions in the membranes can account for the lower proton permeability of various membranes of branch-chained lipids as compared with straight-chained lipids.

MATERIALS AND METHODS

Materials

$Mal_3(Phyt)_2$ was prepared as previously described (Minamikawa and Hato, 1997). Egg yolk phosphatidylcholine (EPC, type V-E) and 1-palmitoyl-2-oleoyl-PC (POPC) were obtained from Sigma (St. Louis, MO). DPhPC and *N*-dansyl-phosphatidylethanolamine (DnsPE) were from Avanti Polar Lipids (Alabaster, AL). MPL (>99%) was from Matreya (Pleasant Gap, PA). Digalactosyldiacylglycerol (DGDG) and sulfoquinovosyldiacylglycerol (SQDG) were from Lipid Products (South Nutfield, Surrey, UK). The molar proportions of the fatty acids of DGDG and SQDG used in the present study were determined by gas chromatography-mass spectrometry technique. After the lipids dissolved in 14 wt % boron trifluoride$_3$-methanol solution were heated at 80°C for 15 min, the obtained methyl esters were analyzed by a Shimadzu GC-17A gas chromatograph and QP-5050 mass spectrometer system using a DB-5 capillary column (0.25-mm inner diameter × 30 m) (J&W Scientific, Folsom, CA). Isothermal runs were performed at 180°C, and fatty acids were identified using authentic standards (Supelco, Bellefonte, PA). The molar proportions of the fatty acids were as follows: DGDG, $C_{18:3}$ (76.7%), $C_{16:0}$ (12.5%), $C_{16:3}$ (4.7%), $C_{18:0}$ (1.8%), $C_{18:1}$ (0.5%), $C_{18:2}$ (3.7%); SQDG, $C_{16:0}$ (34.9%), $C_{18:1}$ (3.2%), $C_{18:0}$ (2.4%), $C_{18:2}$ (12.3%), $C_{18:3}$ (47.1%). The chemical structures of several lipids are shown in Fig. 1. All of the lipids were stored as stock solutions in chloroform/methanol (2:1, v/v) at −20°C, and the absence of impurities in the solutions was checked by thin-layer chromatography. The glycolipids, phospholipids, and SQDG were routinely assayed by the methods of Dubois et al. (1956), Bartlett (1959), and Rosenberg (1963), respectively. A series of *n*-(9-anthroyloxy)fatty acids (*n*AFs): *n*-(9-anthroyloxy)stearic acids (*n*AS, $n = 2, 6, 9, 12$) and 16-(9-anthroyloxy)palmitic acid, 1-palmitoyl-2-(3-(diphenylhexatrienyl)propanoyl)-PC (DPHpPC), and 1-palmitoyl-2-(10-pyrenedecanoyl)-PC (PyrPC) were from Molecular Probes (Eugene, OR). Pyranine (trisodium salt) was from Lambda (Graz, Austria). All of the fluorescent probes were used as received. Deuterium oxide (D_2O) was from Aldrich Chemical Co. (Milwaukee, WI). Organic solvents were spectroscopic grade from Dojindo (Kumamoto, Japan). All other chemicals were guaranteed reagent grade from Wako Pure Chemical Industries (Osaka, Japan).

Vesicle preparation

Multilamellar vesicles (MLVs) were prepared by dispersing the dried lipid thin film in an argon-purged 10 mM phosphate (NaH_2PO_4-Na_2HPO_4) buffer solution (pH 7.0) containing 50 mM K_2SO_4 with vortexing and brief sonication for 5 min in a USC-1 bath-type sonicator (Iuchi Seieido, Osaka, Japan) at 65 W output. Because the vesicles composed of $Mal_3(Phyt)_2$ alone exhibit a significant aggregation in the presence of inorganic salts (Baba et al., 2000), the anionic sulfoglycolipid SQDG was added (10 mol %) to all the lipids used except for MPL (Baba et al., 1999a). Large unilamellar vesicles (LUVs) with a uniform size were prepared by extrusion of frozen-thawed vesicles based on the method described previously (Baba et al., 2000). For the preparation of LUVs entrapping pyranine, a buffer solution containing 0.5 mM pyranine was used. The untrapped pyranine was removed by two passages through a PD-10 column (Pharmacia, Uppsala, Sweden). The average size and polydispersity of vesicles were estimated by dynamic light scattering with an ELS-800TS electrophoretic light-scattering apparatus (Otsuka Electronics, Osaka, Japan).

For *n*AF labeling, vesicle suspensions were mixed with the probe dissolved in dimethylsulfoxide to yield [lipid] + [SQDG] to [probe] molar ratio of 500:1 while vortexing the suspensions. dimethylsulfoxide in suspension was 0.6 vol % or less. The suspensions were incubated at room temperature for at least 2 h before measurements. For phospholipid-type probe labeling, the lipids were mixed with DnsPE, DPHpPC, or PyrPC at [lipid] + [SQDG] to [probe] molar ratios of 200:1, 500:1, or 9:1, respec-

TABLE 1 Net proton/hydroxyl ion permeability of various lipid LUV membranes

Lipid	τ_H/s*	$P_{H/OH}/10^{-4}$ cm s^{-1}	Conditions	References
Linear chained				
EPC/SQDG (9:1)	20 ± 4	17 ± 3	pH 7.0, ΔpH: 0.14, 25°C	This work
EPC†	—	9.6% min^{-1}‡	pH 7.4, ΔpH: 2.4	Foley et al., 1988
	—	$1 - 10^{-1}$	pH 7.2, $\Delta\psi$: 186 mV§	Freisleben et al., 1995
$DC_{16:1}PC$¶	—	18.2	pH 7.0, ΔpH: 0.5, 30°C	Paula et al., 1996
DGDG/SQDG (9:1)	<15	>23	pH 7.0, ΔpH: 0.14, 25°C	This work
DGDG†	—	15.6 ± 6.3% min^{-1}‡	pH 7.4, ΔpH: 2.4	Foley et al., 1988
SBPL	—	27	pH 7.2, ΔpH: 0.2, 25°C	Grzesiek and Dencher, 1986
Branch chained				
DPhPC/SQDG (9:1)	101 ± 30	3.6 ± 1.1	pH 7.0, ΔpH: 0.14, 25°C	This work
DPhPC	—	1.4	pH 7.2, ΔpH: 0.2, 25°C	Grzesiek and Dencher, 1986
$Mal_3(Phyt)_2$/SQDG (9:1)	81 ± 25	4.5 ± 1.4	pH 7.0, ΔpH: 0.14, 25°C	This work
MPL	—	4.5×10^{-2}	pH 7.2, $\Delta\psi$: 186 mV§	Freisleben et al., 1995

*Values are the means ± SD ($n = 3$).
†MLV membranes.
‡Only a relative rate has been described.
§Applied diffusion potential with K^+-valinomycin.
¶Dipalmitoleoyl-PC.

tively, before the vesicle preparation. The final concentrations of total lipids were 0.2 mM. PyrPC was assayed using the extinction coefficient at 343 nm of 5×10^4 cm^{-1} M^{-1} in methanol (Kao et al., 1992).

Proton permeation measurements

Rates of the proton permeation across membranes were estimated by measuring rates of changes in fluorescence intensity of pyranine (Grzesiek and Dencher, 1986) on a JASCO FP-777 spectrofluorometer (Tokyo, Japan) equipped with a thermostated cell holder set at 25 ± 0.1°C. After the removal of carbon dioxide by bubbling of nitrogen gas, small pH gradients (0.14 pH unit) were applied across membranes by injecting a small amount of sulfuric acid under continuous stirring. To abolish a diffusion potential, valinomycin (Sigma) was added into the vesicles before measurements, and the molar ratio of valinomycin to lipid did not exceed 3×10^{-3}. Exciting light (slit bandwidth (SBW) = 3 nm) was changed at a frequency of 1 Hz between 416 nm (isosbestic point) and 450 nm (pH sensitive), and the emission was monitored at 510 nm (SBW = 5 nm). The internal pH was calculated from the ratio of these emission intensities. The pH was calibrated with an HM-30S pH meter (Toa Electronics, Tokyo, Japan).

The net proton/hydroxyl ion permeability coefficients $P_{H/OH}$ were calculated from the decay time of pH gradient τ_H expressed by (Grzesiek and Dencher, 1986):

$$\Delta pH(t) = \Delta pH_0 \exp(-t/\tau_H) \quad (1)$$

in which $\Delta pH(t)$ and ΔpH_0 are pH differences across a membrane at the time t after the addition of an acid and at $t = 0$, respectively. τ_H can be related with $P_{H/OH}$ as follows:

$$\tau_H = (V_m B/A_m)(1/P_{H/OH}[H^+]_0 \ln 10) \quad (2)$$

in which V_m, A_m, and B are the volume and surface area of a vesicle and the buffer capacity, respectively. $[H^+]_0$ is the initial proton concentration of the external phase. As the observed average diameters of all LUVs were 100 ± 10 nm and the size distribution was narrow, the ratio V_m/A_m could be expressed in terms of the vesicle average radius r_m as $V_m/A_m = r_m/3$.

Fluorescence measurements

Fluorescence emission spectra and steady-state fluorescence anisotropy were measured on a Jasco FP-777 spectrofluorometer equipped with a thermostated cell holder (with an accuracy of ±0.1°C). The samples labeled with DnsPE were excited at 340 nm (SBW = 5 nm) and the emission was measured at 528 nm (SBW = 5 nm). For the fluorescence anisotropy measurements of DPHpPC, samples were excited at 366 nm (SBW = 5 nm) and the emission was detected at 430 nm (SBW = 5 nm) using polarizers. The samples labeled with PyrPC were excited at 340 nm (SBW = 3 nm), and the corrected emission intensities for the monomer (398 nm) and the excimer (478 nm) were measured through a slit of 3-nm bandwidth.

Fluorescence lifetimes and anisotropy decays were measured on a Horiba NAES-550 spectrofluorometer (Kyoto, Japan) with a pulsed hydrogen lamp (full width at half maximum: ~ 2 ns) and a thermostated cell holder (with an accuracy of ±0.2°C). The decay curves (resolution: 0.2 or 0.4 ns) were analyzed as double exponentials by using a reiterative deconvolution with the lamp pulse on a Horiba NAES-5×0 nonlinear least square fitting program (see Appendix). The fitness was judged by a reduced χ^2. The samples labeled with *n*AFs were excited through Toshiba UV34 and Hoya U360 filters, and the lifetimes were measured through a Hoya L42 filter. The samples labeled with DnsPE were excited through a Hoya U350 filter, and the lifetimes were measured through a Hoya Y48 filter. For DPHpPC, samples were excited through Toshiba UV31 and Hoya U360 filters, and the lifetimes were measured through a Hoya L42 filter. In the case of anisotropy decay measurements, polarizers were also used. For lifetime measurements of PyrPC excimer, lights of the excitation and emission were passed through MIF-UW345 and MIF-UW479 interference filters (Nihon Sinku Kogaku, Osaka, Japan), respectively. Samples were purged with argon or nitrogen to remove dissolved oxygen before measurements. No corrections for light scattering by vesicles were required.

RESULTS

Proton permeation

The observed decay times of pH gradient τ_H for LUVs of various lipid/SQDG (9:1) at pH 7.0 and 25°C are shown in Table 1. By considering the proton enrichment factor $\exp(-e_0\psi_0/kT)$ at the surface due to the negative surface potential ψ_0 (−15 to −20 mV calculated from 10 mol % of SQDG), the proton concentration at the membrane surface is estimated to be approximately twice that in the

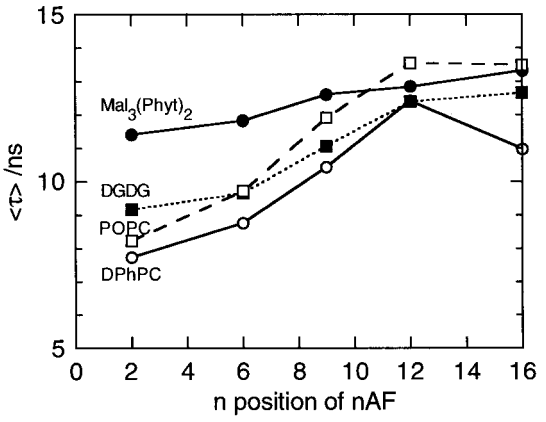

FIGURE 2 Dependence of the average fluorescence lifetime $\langle\tau\rangle$ for *n*AFs on the position of an anthroyloxy fluorophore in various lipid/SQDG (9:1, mol/mol) LUV membranes at 25°C. Data are the means for two experiments ($n = 2$).

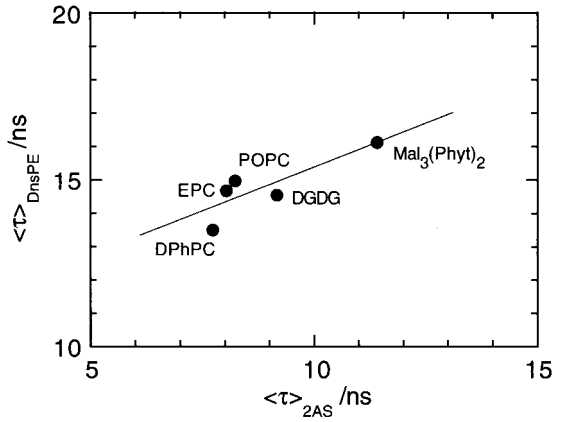

FIGURE 3 Relationship between the average fluorescence lifetimes of DnsPE $\langle\tau\rangle_{DnsPE}$ and 2AS $\langle\tau\rangle_{2AS}$ in various lipid/SQDG (9:1, mol/mol) membranes at 25°C. DnsPE and 2AS were incorporated into MLV and LUV membranes, respectively. Data are the means for two experiments ($n = 2$).

bulk phase. The values of $P_{H/OH}$ for various LUVs were obtained as shown in Table 1. Thus proton permeation rates across membranes of branch-chained lipids are lower than those of straight-chained lipids such as EPC by a factor of ~4.

Degrees of hydration in membranes

Fig. 2 shows the average fluorescence lifetimes $\langle\tau\rangle$ of *n*AFs in various lipid/SQDG membranes at 25°C. Gradients of hydration in membranes can be estimated from the $\langle\tau\rangle$ values of *n*AFs because the fluorophore of *n*AFs is considered to be located in membranes depending on the position number *n*. The location ranges from the membrane-water interface, most probably the glycerol backbone region for 2-(9-anthroyloxy)stearic acid (2AS), to the center of membranes for 16-(9-anthroyloxy)palmitic acid (Abrams et al., 1992), and their $\langle\tau\rangle$ values are more dependent on the concentration of water surrounding the fluorophore than solvent viscosity or dielectric constant (Maçanita et al., 1989; Melo et al., 1991). For POPC, EPC (data not shown but superimposable on the POPC data), DPhPC, and DGDG, the steeper increases in the $\langle\tau\rangle$ value, suggesting decreases in hydration, were observed from the position $n = 2$ to 12. The $\langle\tau\rangle$ values leveled off at $n = 12$ in most cases. Interestingly, *n*AFs in DPhPC/SQDG membrane showed the shortest lifetimes at all depths in the membranes among the lipids examined, suggesting that DPhPC/SQDG membrane has the highest water content among the lipids. $Mal_3(Phyt)_2$/SQDG membrane, however, yielded the longest lifetimes of *n*AFs from the position $n = 2$ to 9. Moreover, the increase in the $\langle\tau\rangle$ value from $n = 2$ to 16 was much less marked than that for other lipids. This result suggests that degrees of hydration and water penetration in $Mal_3(Phyt)_2$/SQDG membrane are the lowest in most parts of the membranes.

Fig. 3 shows the relationship between the $\langle\tau\rangle$ values for 2AS and those for DnsPE in various membranes at 25°C. As the fluorophore of DnsPE is considered to be located near the headgroup region or at the membrane-water interface (Asuncion-Punzalan et al., 1998), its location may be close to that of 2AS. The $\langle\tau\rangle_{2AS}$ value was positively correlated with the $\langle\tau\rangle_{DnsPE}$ value, suggesting that both probes similarly sense the amount of water. Both probes showed the shortest lifetimes for DPhPC/SQDG membrane and conversely the longest lifetimes for $Mal_3(Phyt)_2$/SQDG membrane. The former result can be attributed to more hydration and the latter to less hydration at the membrane-water interfaces.

In addition to the fluorescence lifetime measurements, the deuterium isotope effect on DnsPE fluorescence was also measured as an alternative index (Ho et al., 1995). Fig. 4 shows a plot of the fluorescence intensity ratio (I_D/I_H) of DnsPE in various lipid/SQDG LUVs measured in D_2O or H_2O as a function of the average fluorescence lifetime ratio ($\langle\tau\rangle_D/\langle\tau\rangle_H$) of DnsPE at 25°C. The intensity ratio obtained from each lipid system varied in proportion to its lifetime ratio. DGDG and $Mal_3(Phyt)_2$ showed the lowest ratios; POPC and EPC showed intermediate ratios; DPhPC showed the highest. These results suggest that DnsPE senses the lowest hydration for glycolipid membranes and the highest hydration for DPhPC membrane.

Rotational diffusive motions of DPHpPC in membranes

The rotational diffusive motions of DPHpPC in various lipid/SQDG membranes as well as in MPL membrane were estimated. The parameters are summarized in Table 2.

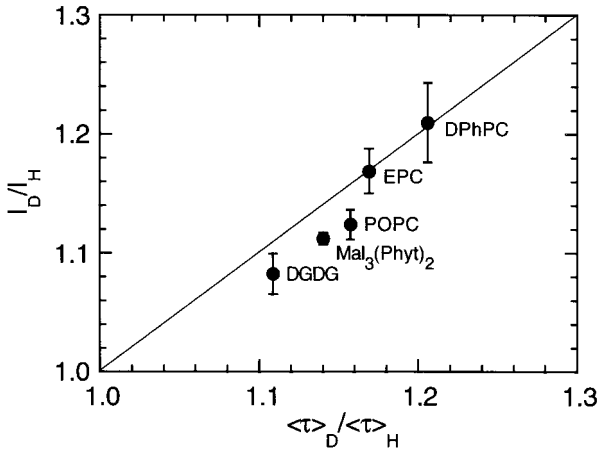

FIGURE 4 Relationship between the fluorescence intensity ratio I_D/I_H of DnsPE in various lipid/SQDG (9:1, mol/mol) MLV membranes prepared in D_2O or H_2O (λ_{ex}, 340 nm; λ_{em}, 528 nm) and the average fluorescence lifetime ratio $\langle\tau\rangle_D/\langle\tau\rangle_H$ of DnsPE in MLV membranes prepared in D_2O or H_2O at 25°C. Data for the intensity ratio are the means ± SD for 10-times repeated measurements for a set of suspensions (n = 2). Data for the lifetime ratio are the means of two experiments.

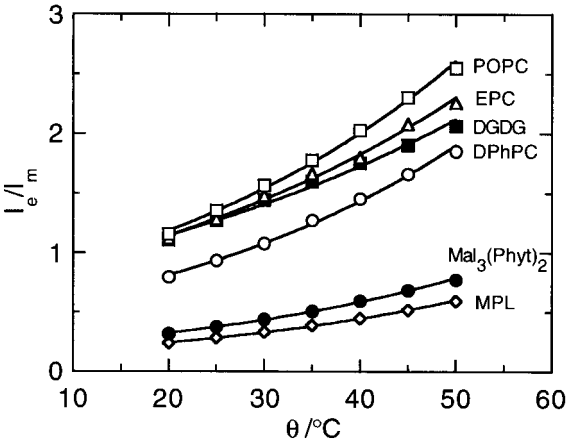

FIGURE 5 Temperature dependence of the intensity ratio of excimer to monomer I_e/I_m of PyrPC in various lipid/SQDG (9:1, mol/mol) LUV membranes. Data are the means of two experiments (n = 2).

The values of the average fluorescence lifetime of DPHpPC $\langle\tau\rangle_{DPHpPC}$ were compared with estimate degrees of hydration near the hydrophobic center of membranes, because the $\langle\tau\rangle_{DPHpPC}$ value depends on the polarity at the deeper region in membranes (Parente and Lentz, 1985). DPhPC/SQDG membrane showed the shortest lifetime indicative of the highest hydration, and conversely MPL membrane showed the longest indicative of the least hydration.

The steady-state fluorescence anisotropies r_{ss} of DPHpPC in branch-chained lipid membranes (DPhPC, $Mal_3(Phyt)_2$, MPL) were higher than those in straight-chained lipid membranes (DGDG, POPC, EPC), indicating greater decreased rotational freedom of the fluorophore in the branch-chained lipid membranes. To obtain the static parameter, i.e., the order parameter of DPHpPC in membranes S and the dynamic parameter, i.e., the rotational diffusion coefficient of DPHpPC in membranes D_w, the fluorescence anisotropy decay data were analyzed in terms of $\langle\phi\rangle$ and r_∞ with average fluorescence lifetimes $\langle\tau\rangle_{DPHpPC}$ by Eqs. A3 and A4 as the first approximation. The S values for $Mal_3(Phyt)_2$/SQDG and MPL membranes are higher than those for straight-chained membranes, however, that for DPhPC/SQDG is comparable with those for POPC/SQDG and EPC/SQDG as seen in Table 2. By comparing the D_w values estimated from Eq. A5, the rotational diffusive motions of DPHpPC in branch-chained lipid membranes were found to be lower than those in straight-chained ones.

Lateral diffusive motions of PyrPC in membranes

Fig. 5 shows the fluorescence intensity ratio of excimer to monomer I_e/I_m of PyrPC as a function of temperature for

TABLE 2 Static and dynamic parameters of DPHpPC and PyrPC in various lipid/SQDG (9:1, mol/mol) LUV membranes

	DPHpPC†						PyrPC	
Lipid*	r_{SS}	r_∞	S	$\langle\tau\rangle_{DPHpPC}$/ns	$\langle\phi\rangle$/ns	D_w/GHz	$A/10^3$ μm^2K^{-1} s^{-1}	E_a/kJ mol^{-1}
Straight chained								
DGDG	0.147 ± 0.009	0.069 ± 0.028	0.42 ± 0.09	6.97 ± 0.07	2.15 ± 1.07	0.094 ± 0.047	0.65 ± 0.10	25.0 ± 0.3
EPC	0.158 ± 0.003	0.098 ± 0.024	0.49 ± 0.06	7.20 ± 0.12	1.79 ± 0.91	0.102 ± 0.052	1.6 ± 0.1	27.2 ± 0.2
POPC	0.167 ± 0.006	0.106 ± 0.022	0.51 ± 0.05	7.23 ± 0.02	1.89 ± 0.92	0.105 ± 0.045	3.6 ± 0.1	29.1 ± 0.0
Branch chained								
DPhPC	0.178 ± 0.006	0.104 ± 0.026	0.51 ± 0.06	6.82 ± 0.03	2.27 ± 1.14	0.077 ± 0.039	6.2 ± 1.0	31.2 ± 0.4
$Mal_3(Phyt)_2$	0.225 ± 0.007	0.157 ± 0.023	0.63 ± 0.05	7.06 ± 0.04	2.74 ± 1.39	0.050 ± 0.025	4.6 ± 0.9	32.2 ± 0.6
MPL‡	0.250 ± 0.008	0.172 ± 0.035	0.66 ± 0.07	8.01 ± 0.04	4.17 ± 3.07	0.031 ± 0.022	3.3 ± 0.2	32.6 ± 0.0

*[Lipid] + [SQDG] = 0.2 mM; [DPHpPC]/{[Lipid] + [SQDG]} = 1/500 (mol/mol); [PyrPC]/{[Lipid] + [SQDG]} = 1/9 (mol/mol).
†Parameters were obtained at 25°C.
‡In the absence of SQDG.

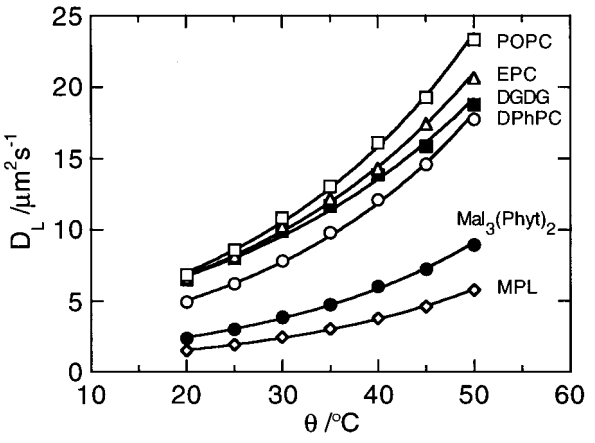

FIGURE 6 Temperature dependence of the lateral diffusion coefficient D_L of PyrPC in various lipid/SQDG (9:1, mol/mol) LUV membranes. The fitting curves were obtained from Eq. 3 by using the values for parameters listed in Table 2. Data are the means of two experiments.

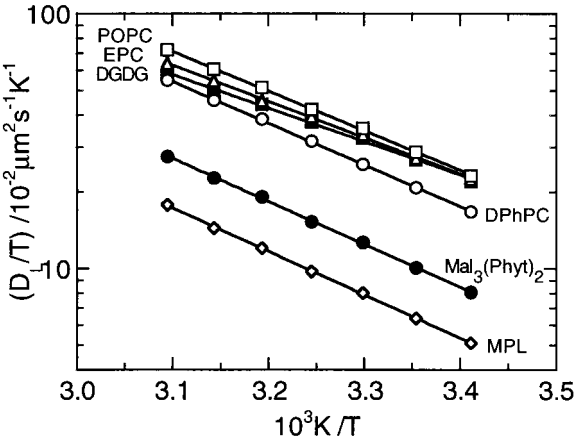

FIGURE 7 Arrhenius plot of $\ln(D_L/T)$ for PyrPC in various lipid/SQDG (9:1, mol/mol) LUV membranes. The fitting curves were obtained from Eq. 3 by using the values for parameters listed in Table 2. Data are the means of two experiments.

various lipids. As all the membranes in the present study are in fluid states at the temperatures examined, PyrPC are considered to be well miscible with the matrix lipids. The I_e/I_m values for branch-chained lipid membranes were found to be lower than those for straight-chained lipid ones.

To evaluate the lateral diffusion coefficients D_L of PyrPC in membranes by using the I_e/I_m values and by Eqs. A6 through A8, the excimer fluorescence lifetimes τ_e of PyrPC and lipid-lipid spacing L need to be estimated. The τ_e values were measured at various temperatures under the condition that excimer emission intensity is higher than that of the monomer and were found to be independent of the membrane composition. The L values were assumed to be independent of temperature and the following values for each lipid were used: $L^2 = 1.0$ nm^2 at 25°C for Mal$_3$(Phyt)$_2$ (Minamikawa and Hato, 1997), $L^2 = 0.75$ nm^2 at 20°C for DGDG (double bond index: ~2.3, Shipley et al., 1973), $L^2 = 0.756$ nm^2 at 25°C for EPC (Lis et al., 1982), and the same value assumed for POPC, $L^2 = 0.8$ nm^2 for DPhPC (Hsieh et al., 1997), and $L^2 = 0.8$ nm^2 for MPL (De Rosa, 1996). The random mixing of the main lipid with SQDG ($L^2 = 0.7$ nm^2) and PyrPC as well as the symmetric distribution of the probe on both sides of the membranes were assumed. Further, although MPL is distributed asymmetrically in the vesicle membrane with most of the PG headgroups facing outside (Komatsu and Chong, 1998), random distribution of PyrPC in MPL monolayer was also assumed. Fig. 6 shows D_L as a function of temperature for all of the lipids used. The D_L values for branch-chained lipid membranes were lower than those for straight-chained lipid ones at the temperatures examined. The D_L values for DPhPC occurred, however, intermediate between the D_L values for straight-chained lipids and those for Mal$_3$(Phyt)$_2$, and became closer to those for straight-chained lipids at higher temperatures.

In the Stokes-Einstein model, the temperature dependence of D_L can be described by the activation energy E_a associated with the effective viscosity,

$$D_L = AT \exp(-E_a/RT) \quad (3)$$

in which A is a temperature-independent constant and R is the gas constant. Fig. 7 shows that the Arrhenius plots of D_L/T display straight lines with correlation coefficients of larger than 0.998. From the slope of these plots, the E_a values of PyrPC diffusion in various lipid membranes were determined to be 25 to 33 kJ/mol as shown in Table 2.

DISCUSSION

Proton permeability

$P_{H/OH}$ values obtained in the present study are in moderate accordance with the reported data of 10^{-3} to 10^{-4} cm/s for several lipid vesicle membranes as shown in Table 1. It should be noted that a small amount of SQDG is considered to have little effect on permeability because it has little influenced membrane conductance (Baba et al., 1999b). The thickness of the hydrophobic region of membranes can be one of the important factors governing proton permeation rates, and this is true when acyl chains are straight and shorter than C_{20} (Paula et al., 1996). Considering the chain lengths of the monopolar lipids examined in the present study are almost the same (mainly saturated C_{16} or unsaturated C_{18}), one would expect that the permeation rates should be almost the same. The previous experiments using planar lipid membranes (Baba et al., 1999b) as well as the present results, however, show that membranes of branch-chained lipids Mal$_3$(Phyt)$_2$ and DPhPC exhibit lower permeability than those of straight-chained lipids such as EPC and soybean phospholipids by a factor of ~4 to 6. Further, membranes of tetraethers (MPL, PLFE) were found

to exhibit exceptionally low proton permeability, which cannot be accounted for solely by the thickness of hydrophobic region (Elferink et al., 1994; Freisleben et al., 1995; Komatsu and Chong, 1998).

It has been reported that proton permeability across lipid membranes is considerably higher than the permeabilities to other monovalent ions and is almost in the range of water permeability: 10^{-2} to 10^{-3} cm/s (Deamer and Nichols, 1989; Paula et al., 1996). Although the coupling between proton and water permeation is less clear, two kinds of water-mediated proton transport mechanisms have been proposed: transient hydrogen-bonded chains of water molecules (Nagle, 1987; Deamer and Nichols, 1989; Marrink et al., 1996; Paula et al., 1996) and passive diffusion of hydrated proton (Paula et al., 1996). The former mechanism assumes the transient formation of strands of water molecules so-called "proton wires," which are connected through the membrane to the opposing water phases and rapidly transport protons from one side to the other (Nagle, 1987; Deamer and Nichols, 1989; Marrink et al., 1996). According to molecular dynamics calculations (Pomès and Roux, 1998), the proton conduction along a proton wire in nonpolar medium includes two complementary steps: the rapid proton translocation along a water chain by way of a proton hopping mechanism and the reorientation of water molecules in the chain. The latter step involves an activation energy of ~33 kJ/mol and is a rate-limiting step for the passage of several protons along the wire. Based on this model, water penetration from membrane-water interface into membranes and molecular motions in membranes seem to govern the formation frequency of the proton wire spanning membranes. Actually, both proton permeability data for the thinner phospholipid membranes and nearly pH-independent conductance data can be explained not by passive diffusion mechanism but by the proton wire mechanism (Nagle, 1987; Paula et al., 1996).

Water penetration (hydration) and molecular motions in membranes, required for the proton wire formation, are considered to be possibly mediated by lipid headgroup fluctuations, lateral diffusive motions, and the migration of gauche-trans-gauche conformations along lipid chains (Haines, 1994). As these conformational changes occur on the time scale of nanoseconds (Yeagle, 1985), nanosecond time-resolved fluorescence spectroscopy is a suitable method to obtain information on molecular motions involved in permeation behavior.

Hydration in membranes

Gradients of hydration in membranes were estimated by use of fluorescent probes: a series of *n*AFs (Maçanita et al., 1989; Melo et al., 1991) and DnsPE (Ho et al., 1995; Asuncion-Punzalan et al., 1998). The lifetime measurements of *n*AFs and DnsPE suggest that $Mal_3(Phyt)_2$/SQDG membrane seems the least hydrated even near the membrane-water interface; in contrast, DPhPC/SQDG membrane seems the most hydrated at all the depths in the membrane. According to Melo et al. (1991), concentrations of water surrounding the fluorophore of *n*AFs [H_2O] can be directly estimated from the relation: $[H_2O] = (\tau_0 - \tau)/k_a\tau\tau_0$ in which τ_0 (=13.5 ns) is the lifetime in the absence of water and k_a is the quenching rate constant. By adopting the k_a value of 5.5×10^6 M^{-1} s^{-1} in dioxane at 25°C (Melo et al., 1991), water concentration could be roughly evaluated as $[H_2O] \sim 2.5$ M for $Mal_3(Phyt)_2$/SQDG membrane-water interface and ~10 M for DPhPC/SQDG. Straight-chained lipid membrane-water interfaces showed $[H_2O] \sim 8.8$ M for POPC/SQDG and EPC/SQDG and ~6.4 M for DGDG/SQDG. Meanwhile, the center of all membranes except DPhPC/SQDG was found to be practically water free. The results from lifetime measurements of DnsPE were consistent with hydration evaluated by 2AS as seen in Fig. 3. Further, because the fluorophore of DnsPE exhibits a deuterium isotope effect on its emission property (Stryer, 1966), degrees of hydration at membrane-water interfaces can be also estimated from the ratios of the fluorescence intensities or lifetimes measured in D_2O and H_2O (Ho et al., 1995). Based on both parameters, $Mal_3(Phyt)_2$/SQDG and DGDG/SQDG membrane-water interfaces seem less hydrated, and conversely DPhPC/SQDG membrane seems much more hydrated as seen in Fig. 4. It is most likely that the difference in headgroup structure largely affects the extent of water penetration into membranes of $Mal_3(Phyt)_2$ and DPhPC because the chain structures of these lipids are similar. These observations are consistent with the structural views on DGDG-water and DPhPC-water systems already reported. DGDG membrane surface from which water tends to be excluded yields a "dry surface" (relatively less hydrated surface), owing to the tightly packed saccharide moieties at the membrane-water interface (McDaniel, 1988). On the contrary, DPhPC membrane surface requires more water molecules than those of straight-chained PCs such as POPC to adopt a "normal" liquid-crystalline lamellar structure, because of the relatively large cross-sectional area in DPhPC (Hsieh et al., 1997). If the former is the case, the low hydration at $Mal_3(Phyt)_2$/SQDG membrane-water interface can be ascribed to the tight packing of saccharide moieties. The extent of water penetration into the deeper region likely reflects the higher density of the interchain free volume into which water molecules can be accommodated. If this is the case, such density in DPhPC/SQDG membrane is the highest among the monopolar lipids examined. On the other hand, the density seems the lowest in $Mal_3(Phyt)_2$/SQDG membrane, which is unlikely because the chains of both lipids are similar, and the molecular occupied area for DPhPC monolayer is smaller than that for $Mal_3(Phyt)_2$ under a constant surface pressure (Baba et al., 1999b). It is most likely that the bulkier saccharide moiety may act as a barrier and lower the accessibility of water molecules to the interchain free volume.

The order of decreasing hydration in membranes is obviously inconsistent with the order of decreasing proton permeability. Therefore, the lower proton permeability of branch-chained lipid membranes cannot be ascribed solely to hydration in membranes.

Lipid molecular motions in membranes

For straight-chained lipids, rotational diffusion coefficients of DPHpPC and lateral diffusion coefficients of PyrPC were relatively large as seen in Table 1 and Figs. 6 and 7. The molecular motions in DGDG membrane seem somewhat low compared with those of POPC and EPC, and this is possibly due to the laterally forming hydrogen-bond network among the headgroups. For branch-chained lipids, the tetraether MPL membrane showed the most restricted molecular motions among the lipids examined. The D_L values for MPL were 2.4, 3.8, and 5.8 $\mu m^2/s$ at 30, 40, and 50°C, respectively, whereas those for total lipids from *Thermoplasma acidophilum* containing MPL have been reported to be 0.5 to 0.6, 0.99, and 2 $\mu m^2/s$ at 30, 40, and 50°C, respectively, on the basis of ^{31}P-NMR technique (Jarrel et al., 1998). As the D_L values estimated by PyrPC excimer formation technique are usually about an order of magnitude larger than those estimated by other techniques (Tocanne et al., 1994), the present result for MPL is not irrelevant to the ^{31}P-NMR results. The very restricted motions of PyrPC were also reported in another tetraether lipid PLFE membrane (Kao et al., 1992). $Mal_3(Phyt)_2$/SQDG membrane also showed highly restricted motions. These findings suggest that the higher intermolecular constraint is imposed on lipid molecules in the branch-chained membranes. ^{2}H-NMR technique has provided important information on dynamic properties of branch-chained lipid membranes and showed that methyl branches in a phytanyl chain reduce the segmental motion, e.g., gauche-trans-gauche kink formation at the tertiary carbons and lower the rate of the motion of the phytanyl chain itself (Degani et al., 1980; Stewart et al., 1990). The E_a values for PyrPC in branch-chained lipid membranes are somewhat higher than those in straight-chained lipid ones as seen from Table 2. This may be due to the steric hindrance of methyl branches against the lateral diffusive motions of PyrPC. These restricted motions in branch-chained membranes should lead to the reduction of translocational and reorientational motions of water molecules responsible for proton permeation.

It should be noted that DPhPC/SQDG membrane showed molecular motions as high as 70 to 80% of the motional rates observed in straight-chained lipid membranes at 25°C. DPhPC membranes were found to be loosely packed compared with tetraether lipid ones by fluorescence measurements (Khan and Chong, 2000) and molecular dynamics calculations (Gabriel and Chong, 2000). These findings support the view that molecular motions in DPhPC membranes are higher than those in MPL ones. However, the difference in motions between DPhPC and $Mal_3(Phyt)_2$ cannot be ascribed solely to interchain packing because the chains of both lipids are similar as mentioned above. The bulkier saccharide moiety of $Mal_3(Phyt)_2$ may partly reduce motions, and this is probably due to the formation of hydrogen-bond network among headgroups.

If one assumes that water penetration into membranes is governed by lateral diffusive motions of lipids (Haines, 1994) and a certain fraction of water permeability P_{H2O} is involved in a "proton wire" formation, the relative proton permeability for various membranes at 25°C can be roughly estimated from the relation: $P_{H/OH} \propto P_{H2O} \propto D_L/L^4$ (Haines, 1994) as 100 for EPC/SQDG, 105 for POPC/SQDG, 100 for DGDG/SQDG, 70 for DPhPC/SQDG, and 20 for $Mal_3(Phyt)_2$/SQDG, respectively. Obviously, the value for $Mal_3(Phyt)_2$ is reasonable to explain the lower proton permeability compared with that for EPC by a factor of ~4, although the value for DPhPC is too large because of its large lateral motion in membranes. In addition to this dynamic view, it can be speculated that bulky methyl branches showing "lateral interdigitation" (Dannenmuller et al., 2000) may prevent water molecules from forming "proton wires" spanning a membrane, resulting in a reduction of an efficient proton transport. According to molecular dynamics calculations (Marrink et al., 1996), the energy barrier of the formation of a "proton wire" spanning a membrane was estimated to be >100 kJ/mol, indicating that a complete "proton wire" formation is a rare phenomenon. The presence of bulky branches may lower the formation frequency of such molecular assemblies. Further molecular dynamics studies would provide more information on the behavior of water assemblies in branch-chained lipid membranes. At the present stage, however, it can be concluded that the restricted motion of chain segments rather than lower hydration accounts for the lower proton permeability of branch-chained lipid membranes.

APPENDIX

The total fluorescence decay $I(t)$ is expressed with exponential decay functions with the fractional amplitude α_i and the fluorescence lifetime τ_i for the i-th component:

$$I(t) = \Sigma\alpha_i \exp(-t/\tau_i) \quad \text{(A1)}$$

The average fluorescence lifetime $\langle\tau\rangle$ is calculated from Eq. A2:

$$\langle\tau\rangle = \Sigma\alpha_i \tau_i^2/\Sigma\alpha_i \tau_i \quad \text{(A2)}$$

According to the wobbling-in-cone model as a hindered rotational motion of a fluorophore, the fluorescence anisotropy decay $r(t)$ is expressed as (Kawato et al., 1977):

$$r(t) = (r_0 - r_\infty)\exp(-t/\langle\phi\rangle) + r_\infty \quad \text{(A3)}$$

in which r_0 and r_∞ are the anisotropies at $t = 0$ and at $t \to \infty$, respectively. $\langle\phi\rangle$ is a single-component rotational correla-

tion time. The value of r_0 was assumed to be 0.40. The order parameter S of the fluorophore is related to r_∞ as follows:

$$S^2 = r_\infty/r_0 = [x(1 + x)]^2/4. \quad \text{(A4)}$$

The rotational diffusion coefficient D_w can be estimated as follows (Lipari and Szabo, 1980):

$$D_w\langle\phi\rangle(1 - S^2) = -\frac{x^2(1 + x)^2\{\ln[(1 + x)/2] + (1 - x)/2\}}{[2(1 - x)]} + (1 - x)(6 + 8x - x^2 - 12x^3 - 7x^4)/24. \quad \text{(A5)}$$

For PyrPC molecules which perform a random walk in a plane, by taking steps of length L corresponding to the average lipid-lipid spacing in membranes, and at PyrPC stepping frequency f, the lateral diffusion coefficient of PyrPC D_L is given by:

$$D_L = fL^2/4 \quad \text{(A6)}$$

and

$$f = \langle N\rangle(1/\kappa)(I_e/I_m)(k_m/k_e)(1/\tau_e) \quad \text{(A7)}$$

in which κ is a constant characteristic for the probe used, (I_e/I_m) is the ratio of the excimer emission intensity I_e to the monomer one I_m, and (k_m/k_e) is the ratio of the radiative decay constant of the excited monomer k_m to that of the excimer k_e. The values of κ and (k_m/k_e) for PyrPC were assumed to be 0.8 and 0.1, respectively (Galla and Sackmann, 1974). τ_e is the excimer lifetime. $\langle N\rangle$ is the average step number between collisions of probe molecules and expressed in terms of the molar fraction of the probe X_{PyrPC} as follows (Galla et al., 1979):

$$\langle N\rangle = (2/\pi X_{PyrPC})\ln(2/X_{PyrPC}). \quad \text{(A8)}$$

We wish to thank Dr. Y. Tsumura (National Institute of Health Sciences (NIHS), Osaka, Japan) for fatty acid analyses, Dr. H. Saito (NIHS) for his help and advice with time-resolved fluorescence measurements, and Dr. H. Komatsu (Thomas Jefferson University, PA) for his valuable comments and also for reading the manuscript. T.B. is indebted to the Science and Technology Agency, Japan for its grant.

This work was performed as part of R&D Projects of Industrial Science and Technology Frontier Program (physical properties of glycolipid/membrane protein assemblies) supported by AIST, the Ministry of International Trade and Industry, Japan.

REFERENCES

Abrams, F. S., A. Chattopadhyay, and E. London. 1992. Determination of the location of fluorescent probes attached to fatty acids using parallax analysis of fluorescence quenching: effect of carboxyl ionization state and environment on depth. *Biochemistry.* 31:5322–5327.

Asuncion-Punzalan, E., K. Kachel, and E. London. 1998. Groups with polar characteristics can locate at both shallow and deep locations in membranes: the behavior of dansyl and related probes. *Biochemistry.* 37:4603–4611.

Baba, T., H. Minamikawa, M. Hato, A. Motoki, M. Hirano, D. Zhou, and K. Kawasaki. 1999a. Synthetic phytanyl-chained glycolipid vesicle membrane as a novel matrix for functional reconstitution of cyanobacterial photosystem II complex. *Biochem. Biophys. Res. Commun.* 265: 734–738.

Baba, T., Y. Toshima, H. Minamikawa, M. Hato, K. Suzuki, and N. Kamo. 1999b. Formation and characterization of planar lipid bilayer membranes from synthetic phytanyl-chained glycolipids. *Biochim. Biophys. Acta.* 1421:91–102.

Baba, T., L.-Q. Zheng, H. Minamikawa, and M. Hato. 2000. Interglycolipid membrane interactions: pH-dependent aggregation of nonionic synthetic glycolipid vesicles. *J. Colloid Interface Sci.* 223:235–243.

Bartlett, G. R. 1959. Phosphorus assay in column chromatography. *J. Biol. Chem.* 234:466–468.

Choquet, C. G., G. B. Patel, T. J. Beveridge, and G. D. Sprott. 1994. Stability of pressure-extruded liposomes made from archaeobacterial ether lipids. *Appl. Microbiol. Biotechnol.* 42:375–384.

Dannenmuller, O., K. Arakawa, T. Eguchi, K. Kakinuma, S. Blanc, A.-M. Albrecht, M. Schumtz, Y. Nakatani, and G. Ourisson. 2000. Membrane properties of archaeal macrocyclic diether phospholipids. *Chem. Eur. J.* 6:645–654.

Deamer, D. W., and J. W. Nichols. 1989. Proton flux mechanisms in model and biological membranes. *J. Membr. Biol.* 107:91–103.

Degani, H., A. Danon, and S. R. Caplan. 1980. Proton and carbon-13 nuclear magnetic resonance studies of the polar lipids of *Halobacterium halobium. Biochemistry.* 19:1626–1631.

De Rosa, M. 1996. Archaeal lipids: structural features and supramolecular organization. *Thin Solid Films.* 284–285:13–17.

Dubois, M., K. A. Gilles, J. K. Hamilton, P. A. Rebers, and F. Smith. 1956. Colorimetric method for determination of sugars and related substances. *Anal. Chem.* 28:350–356.

Elferink, M. G. L., J. G. de Wit, R. Demel, A. J. M. Driessen, and W. N. Konings. 1992. Functional reconstitution of membrane proteins in monolayer liposomes from bipolar lipids of *Sulfolobus acidocaldarius. J. Biol. Chem.* 267:1375–1381.

Elferink, M. G. L., J. G. de Wit, A. J. M. Driessen, and W. N. Konings. 1994. Stability and proton-permeability of liposomes composed of archaeal tetraether lipids. *Biochim. Biophys. Acta.* 1193:247–254.

Foley, A. A., A. P. R. Brain, P. J. Quinn, and J. L. Harwood. 1988. Permeability of liposomes composed of binary mixtures of monogalactosyldiacylglycerol and digalactosyldiacylglycerol. *Biochim. Biophys. Acta.* 939:430–440.

Freisleben, H.-J., K. Zwicker, P. Jezek, G. John, A. Bettin-Bogutzki, K. Ring, and T. Nawroth. 1995. Reconstitution of bacteriorhodopsin and ATP synthase from *Micrococcus luteus* into liposomes of the purified main tetraether lipid from *Thermoplasma acidophilum*: proton conductance and light-driven ATP synthesis. *Chem. Phys. Lipids.* 78:137–147.

Gabriel, J. L., and P. L. G. Chong. 2000. Molecular modeling of archaebacterial bipolar tetraether lipid membranes. *Chem. Phys. Lipids.* 105: 193–200.

Galla, H.-J., W. Hartmann, U. Theilen, and E. Sackmann. 1979. On two-dimensional passive random walk in lipid bilayers and fluid pathways in biomembranes. *J. Membr. Biol.* 48:215–236.

Galla, H.-J., and E. Sackmann. 1974. Lateral diffusion in the hydrophobic region of membranes: use of pyrene excimers as optical probes. *Biochim. Biophys. Acta.* 339:103–115.

Gambacorta, A., A. Gliozzi, and M. de Rosa. 1995. Archaeal lipids and their biotechnological applications. *World J. Microbiol. Biotechnol.* 11: 115–131.

Grzesiek, S., and N. A. Dencher. 1986. Dependency of ΔpH-relaxation across vesicular membranes on the buffering power of bulk solutions and lipids. *Biophys. J.* 50:265–276.

Haines, T. H. 1994. Water transport across biological membranes. *FEBS Lett.* 346:115–122.

Hato, M., H. Minamikawa, K. Tamada, T. Baba, and Y. Tanabe. 1999. Self-assembly of synthetic glycolipid/water systems. *Adv. Colloid Interface Sci.* 80:233–270.

Ho, C., S. J. Slater, and C. D. Stubbs. 1995. Hydration and order in lipid bilayers. *Biochemistry.* 34:6188–6195.

Hsieh, C.-H., S.-C. Sue, P.-C. Lyu, and W.-G. Wu. 1997. Membrane packing geometry of diphytanoylphosphatidylcholine is highly sensitive to hydration: phospholipid polymorphism induced by molecular rearrangement in the headgroup region. *Biophys. J.* 73:870–877.

Jarrel, H. C., K. A. Zukotynski, and G. D. Sprott. 1998. Lateral diffusion of the total polar lipids from *Thermoplasma acidophilum* in multilamellar liposomes. *Biochim. Biophys. Acta.* 1369:259–266.

Kao, Y. L., E. L. Chang, and P. L.-G. Chong. 1992. Unusual pressure dependence of the lateral motion of pyrene-labeled phosphatidylcholine in bipolar lipid vesicles. *Biochem. Biophys. Res. Commun.* 188: 1241–1246.

Kawato, S., K. Kinoshita, Jr., and A. Ikegami. 1977. Dynamic structure of lipid bilayers studied by nanosecond fluorescence techniques. *Biochemistry.* 16:2319–2324.

Khan, T. K., and P. L.-G. Chong. 2000. Studies of archaebacterial bipolar tetraether liposomes by perylene fluorescence. *Biophys. J.* 78: 1390–1399.

Komatsu, H., and P. L.-G. Chong. 1998. Low permeability of liposomal membranes composed of bipolar tetraether lipids from thermoacidophilic archaebacterium *Sulfolobus acidocaldarius. Biochemistry.* 37: 107–115.

Lipari, G., and A. Szabo. 1980. Effect of liberational motion on fluorescence depolarization and nuclear magnetic resonance relaxation in macromolecules and membranes. *Biophys. J.* 30:489–506.

Lis, L. J., M. McAlister, N. Fuller, R. P. Rand, and V. A. Parsegian. 1982. Interactions between neutral phospholipid bilayer membranes. *Biophys. J.* 37:657–666.

Maçanita, A. L., F. P. Costa, S. M. B. Costa, E. C. Melo, and H. Santos. 1989. The 9-anthroate chromophore as a fluorescent probe for water. *J. Phys. Chem.* 93:336–343.

Marrink, S. J., F. Jähnig, and H. C. J. Berendsen. 1996. Proton transport across transient single-file water pores in a lipid membrane studied by molecular dynamics simulations. *Biophys. J.* 71:632–647.

McDaniel, R. V. 1988. Neutron diffraction studies of digalactosyldiacylglycerol. *Biochim. Biophys. Acta.* 940:158–164.

Melo, E. C. C., S. M. B. Costa, A. L. Maçanita, and H. Santos. 1991. The use of the *n*-(9-anthroyloxy) stearic acids to probe the water content of sodium dodecyl sulfate, dodecyltrimethylammonium chloride, and Triton X-100 micelles. *J. Colloid Interface Sci.* 141:439–453.

Minamikawa, H., and M. Hato. 1997. Phase behavior of synthetic phytanyl-chained glycolipid/water systems. *Langmuir.* 13:2564–2571.

Nagle, J. F. 1987. Theory of passive proton conductance in lipid bilayers. *J. Bioenerg. Biomembr.* 19:413–426.

Parente, R. A., and B. R. Lentz. 1985. Advantages and limitations of 1-palmitoyl-2-[[2-[4-(6-phenyl-*trans*-1, 3, 5-hexatrienyl) phenyl]ethyl]-carbonyl]-3-*sn*-phosphatidylcholine as a fluorescent probe. *Biochemistry.* 25:1021–1026.

Paula, S., G. Volkov, N. van Hoek, T. H. Haines, and D. W. Deamer. 1996. Permeation of protons, potassium ions, and small polar molecules through phospholipid bilayers as a function of membrane thickness. *Biophys. J.* 70:339–348.

Pomès, R., and B. Roux. 1998. Free energy profiles for H^+ conduction along hydrogen-bonded chains of water molecules. *Biophys. J.* 75: 33–40.

Rosenberg, A. 1963. A comparison of lipid patterns in photosynthesizing and non-photosynthesizing cells of *Euglena gracilis. Biochemistry.* 2:1148–1154.

Shipley, G. G., J. P. Green, and B. W. Nichols. 1973. The phase behavior of monogalactosyl, digalactosyl, and sulphoquinovosyl diglycerides. *Biochim. Biophys. Acta.* 311:531–544.

Stewart, L. C., M. Kates, I. H. Ekiel, and I. C. P. Smith. 1990. Molecular order and dynamics of diphytanylglycerol phospholipids: a ^2H and ^{31}P-NMR study. *Chem. Phys. Lipids.* 54:115–129.

Stryer, L. 1966. Excited-state proton-transfer reactions: a deuterium isotope effect on fluorescence. *J. Am. Chem. Soc.* 88:5708–5712.

Swaine, M., J.-R. Brisson, G. D. Sprott, F. P. Cooper, and G. B. Patel. 1997. Identification of β-L-gulose as the sugar moiety of the main polar lipid *Thermoplasma acidophilum. Biochim. Biophys. Acta.* 1345:56–64.

Tocanne, J.-F., L. Dupou-Cézanne, and A. Lopez. 1994. Lateral diffusion of lipids in model and natural membranes. *Prog. Lipid Res.* 33:203–237.

Van de Vossenberg, J. L. C. M., A. J. M. Driessen, and W. N. Konings. 1998. The essence of being extremophilic: the role of the unique archaeal membrane lipids. *Extremophiles.* 2:163–170.

Yamauchi, K., K. Doi, M. Kinoshita, F. Kii, and H. Fukuda. 1992. Archaebacterial lipid models: highly salt-tolerant membranes from 1,2-diphytanylglycero-3-phosphocholine. *Biochim. Biophys. Acta.* 1110: 171–177.

Yamauchi, K., K. Doi, Y. Yoshida, and M. Kinoshita. 1993. Archaebacterial lipids: highly proton-impermeable membranes from 1,2-diphytanyl-*sn*-glycero-3-phosphocholine. *Biochim. Biophys. Acta.* 1146: 178–182.

Yeagle, P. L. 1985. Cholesterol and the cell membrane. *Biochim. Biophys. Acta.* 822:267–287.